Adsorption of Li, Cs, and O on CdTe

J. Gordon and P. Morgen
Physics Department, Odense University, Campusvej 55, Odense M, DK-5230, Denmark

H. Shechter
Physics Department and Solid State Institute, Technion—Israel Institute of Technology, Haifa 32000, Israel

M. Folman
Chemistry Department and Solid State Institute, Technion—Israel Institute of Technology, Haifa 32000, Israel
(Received 8 February 1995)

The adsorption of Li and Cs on CdTe(100) single crystals was investigated using different surface sensitive electron spectroscopies. Low-energy electron diffraction shows a number of surface reconstructions of the clean surfaces, influenced by the Cd/Te ratio. Deposition of Li shows a constant sticking probability, while Cs has a variable sticking probability, characteristic of island growth coalescing at a coverage of a monolayer. Li and Cs both form amorphous monoatomic layers. Large work-function changes of the CdTe surface as a function of Li and of Cs coverage were found at the initial stages of adsorption, indicating that Cs and Li atoms are to a large extent ionized on the surface (100) plane. The initial dipole moments for Cs and for Li were calculated with the Helmholtz equation $\mu_{\mathrm{Cs},\theta\to 0}\approx 26$ D and $\mu_{\mathrm{Li},\theta\to 0}\approx 3.2$ D and using Topping plots $\mu_{0,\mathrm{Cs}}=127.2$ D and $\mu_{0,\mathrm{Li}}=4.22$ D. Adsorption of oxygen on the cesium-covered surface raises the work function by $\Delta\phi=0.5\pm 0.05$ eV. Reflection-electron energy-loss spectra of the cesiated CdTe(100) surface at $E_p=100$ eV, recorded at a low temperature (96 K), show a characteristic Cs two-dimensional surface plasmon, $\hbar\omega_s$ at 2.05 eV, which disappears with rising temperature. During Cs growth a loss is observed at 26.6 eV which is assigned to Cs 5*s* core-level transitions.

I. INTRODUCTION

The adsorption of alkali metals and oxygen, to lower the work function (ϕ) of a metal or a semiconductor surface, has been the subject of numerous studies. In particular, the activation of certain semiconductor surfaces to a state of negative electron affinity, in which the bottom of the conduction band is brought above the vacuum level, has been of interest in the last two decades as a means for preparing photoemitters.[1] Examples of some systems are (Na-O)/W(112),[2] (K-O)/Ag(100),[3,4] (Cs-O)/GaAs,[5] and Cs/CdTe.[6–10] Applications of such system are also found in catalysis and in thermionic devices. In this context extensive studies have been reported on Si(Cs-O) and on systems of the III-V group of semiconductors, such as GaAs(Cs-O), InP(Cs-O), and GaP/Cs. These systems are characterized by a photoemission threshold near the bandgap energy of the semiconductor. With the goal of adjusting the band gap for a specific application, some of the ternaries of the III-V group, $In_{1-x}Ga_xAs$(Cs-O), and $In_{1-x}As_xP$(Cs-O) were used as photoemitters. The use of ternaries allows a shift of the onset for efficient photoemission toward the infrared region of the spectrum and excellent detectors for the near-infrared region were constructed.[7] There is also a third group of infrared detectors based on the II-VI compounds, CdTe and $Hg_{1-x}Cd_xTe$. These materials form high-quality systems (the lattice mismatch between CdTe and $Hg_{1-x}Cd_xTe$ is only 0.3%) with great potential for applications in the field of photoelectronic devices operating at wavelengths longer than those possible with the III-V semiconductors.[8,9] Surfaces of CdTe were scarcely studied in the past in this context and information about these systems (alkali-metal/CdTe) is almost nonexistent in the literature. As far as we know, only one investigation was reported.[10] The present paper follows our previous one[6] on Cs/CdTe. Here we concentrate on adsorption data obtained by Auger-electron spectroscopy (AES), low-energy electron diffraction (LEED), work-function measurements, and reflection-electron energy-loss spectroscopy (REELS) measurements during the deposition of Li, Cs, and the subsequent adsorption of oxygen on a CdTe(100) surface.

II. EXPERIMENT

Low-energy electron diffraction (LEED), Auger electron spectroscopy (AES), adsorption-dependent work-function change, and reflection electron energy loss spectroscopy (REELS) were employed in this investigation.

The samples used were *p*-type CdTe single crystals, grown by the vertical Bridgman method [oriented to within $\pm 0.5°$, in the (100) direction]. They were *p* type with bulk-carrier densities of 2×10^{15} cm^{-3}. This value was measured by the Hall effect, C/V, and I/V techniques. The preparation of the (100-oriented surfaces was done by mechanically polishing the single crystal with 0.3-μm aluminum oxide. The crystal was subsequently rinsed with deionized water, and then cleaned with trichloroethylene, acetone, and methanol in an ultrasonic cleaner. Finally, prior to insertion into the UHV chamber, the surface was etched with a solution of bro-

0163-1829/95/52(3)/1852(7)/$06.00 ©1995 The American Physical Society

mine in methanol (2% in volume) to remove the uppermost layer.[11] These surfaces were subsequently sputter-cleaned *in situ* by means of an Ar^+ ion beam of 800 eV and thermally annealed to 250 °C for 5 min. In most cases, such a procedure gave a well-defined CdTe(100)(1×1) LEED pattern with no traces of impurities (as monitored by AES). The surface treatment, modification, and characterization were performed in an ultrahigh-vacuum system (6×10^{-11} Torr base pressure) equipped with a LEED retarding grid detector, AES, and electronics for the measurements of the work-function changes by the retarding field method[12] with a ±50-mV resolution. A cold finger allowed us to cool the samples to 96 K with LN_2. Resistive heating was performed with a tungsten filament wire located behind the back of the sample in the arm of the sample manipulator. The sample temperature was determined with a Chromel-Alumel thermocouple spot-welded near the back of the CdTe sample, on the sample holder. The experimental system also allowed admission of controlled amounts of molecular oxygen (O_2). Cs and Li were evaporated from commercially obtained alkali-metal sources (SAES GETTERS S.p.A., Italy), each thoroughly outgassed and enclosed in a cell made of stainless steel with a hole covered by a rotatable shutter. A schematic drawing of the experimental system is shown in Fig. 1. The background pressure during alkali-metal deposition was kept below 10^{-9} Torr.

III. RESULTS

A. Auger-electron spectroscopy: Li and Cs adsorption

In Fig. 2 is shown a typical Auger peak-to-peak plot of lithium (Li_{KLL} 43 eV) and cesium (Cs_{MNN} 536 eV) versus deposition time, obtained during growth of monoatomic layers on CdTe(100) substrate at room temperature. The results for Cs (Ref. 6) are given here for comparison. The growth of Cs shows a variable sticking coefficient (s_{Cs}),

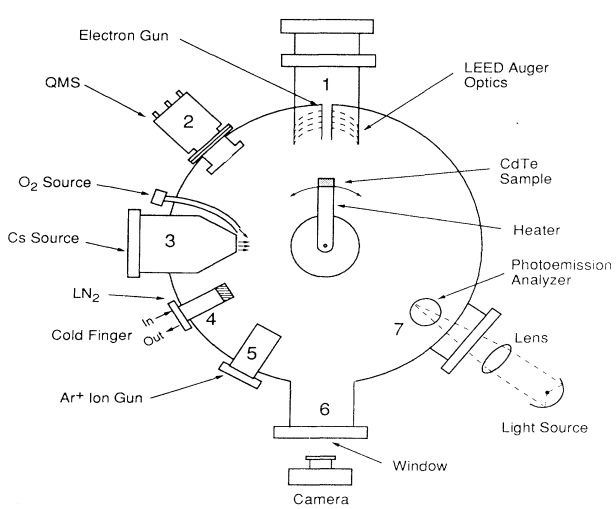

FIG. 1. Schematics of the experimental chamber.

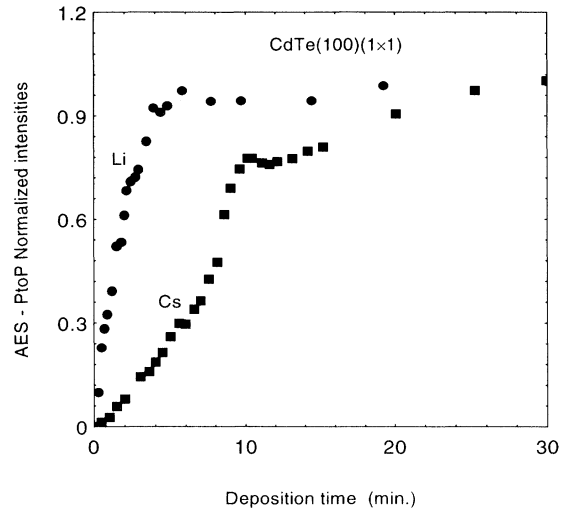

FIG. 2. Intensities of the AES signals (peak to peak) as a function of Li and Cs deposition times. Li *KLL* transition at 43 eV, Cs *MNN* transition at 563 eV, Cs curve from Ref. 6 given for comparison.

which is consistent with the growth of a Cs layer by the formation of two-dimensional (2D) clusters which coalesce near monolayer coverage.[5,13] In contrast, the Li sticking coefficient (s_{Li}) is constant as shown by the linear dependence of the Auger intensities (Li_{KLL} 43 eV) versus deposition time (AI-*t* plot). The fractional coverage of Li and Cs was assessed by AES and the monolayer completion is taken at the break point in the slopes of the AI-*t* plots. Throughout this work we define a Cs monolayer (ML) as 4.6×10^{14} atoms cm^{-2} which is close to the density of a saturated Cs monolayer on most metals and semiconductors[13–15] and a Li ML as 1.7×10^{15} atoms cm^{-2}. The Li ML is calculated, to a first approximation, from the break point in the corresponding AI-*t* plot (Fig. 2), from the ratio between the radii of both ionic species $r^+_{Cs}/r^+_{Li}=1.95$,[16] and by assuming a direct proportionality in the densities of both disordered monolayers.

B. Low-energy electron diffraction: Clean and akali-metal-deposited surfaces

The low-index polar faces CdTe(100) and CdTe(111) were studied with LEED. Initially, no pattern was obtained from the specimens as the surfaces were contaminated with a thin layer of carbon. The surfaces were cleaned *in situ* by sputtering with Ar^+ at low energy, 800 eV for 10 min, after which a weak electron-diffraction pattern of the nonreconstructed surface (which was superimposed on a bright background) appeared in most cases. All LEED observations were done using primary electron energies in the range of 12–60 eV. Well-defined LEED patterns of unreconstructed CdTe(100) and CdTe(111) were obtained only after subsequent thermal annealing of the samples to 250 °C for 5 min. Typical LEED patterns obtained from these surfaces are shown in Figs. 3(a) and 3(b). In some instances, although the

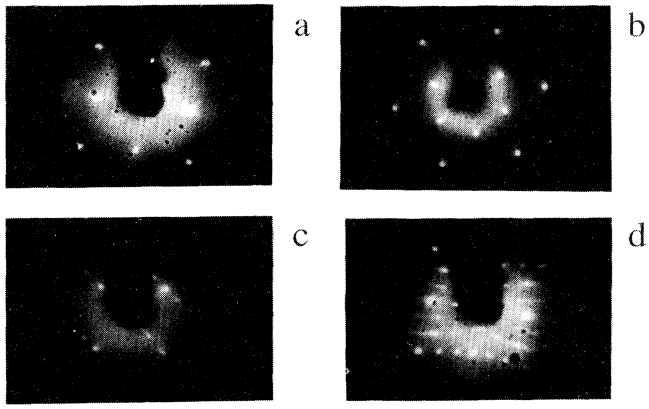

FIG. 3. (a) CdTe(100) unreconstructed surface at 40 eV, (b) CdTe(111) unreconstructed surface at 25 eV, (c) CdTe(100)(3×1)$R45°$ at 40 eV and (d) CdTe(100)(3×3) at 40 eV.

same surface treatment was performed, different surface structures were obtained. This behavior is most probably related to the different stoichiometries of the top surface layers, which results from bombardment with Ar^+ ions during the sputtering process. This type of stoichiometry-dependent reconstruction of the surface was obtained in the past also for the homologous faces in GaAs.[17] The different reconstructions which were observed in this work are CdTe(100)(3×1) and CdTe(111)(2×2), already reported in the literature,[18] and CdTe(100)(3×1)$R45°$ and CdTe(100)(3×3), which are reported here in Figs. 3(c) and 3(d), respectively.

LEED patterns during growth of a monolayer of Cs and of a monolayer of Li obtained for different Cs and Li fractional coverages, for $0 \leq \theta_{Cs}, \theta_{Li} \leq 1$ are shown in Figs. 4 and 5. The low-energy diffraction patterns for the Cs film growth were taken at 40 eV primary energy and at 13 eV primary energy for Li. Both Li and Cs were studied only on the CdTe(100)(1×1) surface. During alkali-metal deposition the background intensity increased, until the diffraction spots from the substrate disappeared completely (in the case of Cs) or remained just perceptible in the case of Li. No appearance of additional diffraction spots was observed during the deposition stages. This indicates that Cs and Li grow on CdTe(100) in a disordered way, resulting in an amorphous monolayer. In the case of Li deposition the diffraction spots were discernible even at a coverage of $\theta_{Li}=1$, in contrast to the case of Cs deposition where diffraction spots vanished at $\theta_{Cs}=0.22$. This is attributed to the different electron structures of Li and Cs and to the difference in ionic radii.[16] In lithium the 2*s* electron, the only one which can interact easily at these low energies, is partially transferred to the CdTe substrate leaving the Li(2*s*) level almost empty. In Cs there are a number of electrons that can scatter and screen the diffracted electrons from this substrate, even if the 6*s* electron is partially transferred to the CdTe. Therefore, a lithium monolayer causes less attenuation to the energy of the CdTe surface diffracted electrons than a cesium monolayer.

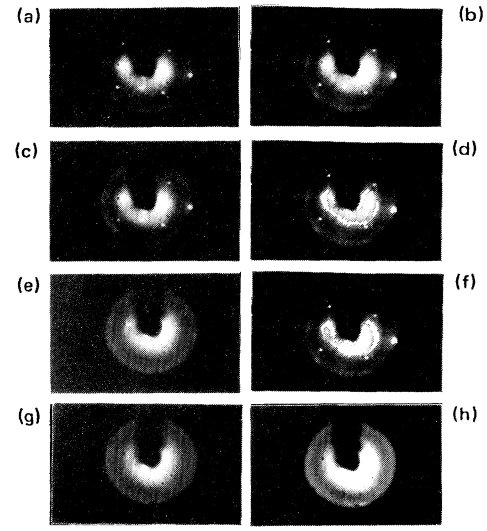

FIG. 4. LEED patterns taken during the growth of Cs on the unreconstructed CdTe(100) surface at 40 eV. (a) $\theta_{Cs}=0$, (b) $\theta_{Cs}=0.06$, (c) $\theta_{Cs}=0.11$, (d) $\theta_{Cs}=0.22$, (e) $\theta_{Cs}=0.33$, (f) $\theta_{Cs}=0.39$, (g) $\theta_{Cs}=0.50$, and (h) $\theta_{Cs}=1$.

C. Work-function changes: Li, Cs, and oxygen adsorption

During deposition of Cs and Li, and also during subsequent adsorption of oxygen, work-function changes were measured by the ac-retarding field method for the unreconstructed CdTe(100) surface. The results for Cs (Ref. 6) are given here for comparison. Work-function changes versus lithium and cesium coverage (θ) of the CdTe(100)(1×1) surface are shown in Fig. 6. While the Cs curve exhibits a fast initial drop, $d(\Delta\phi)/d\theta_{Cs} \approx 22.4$

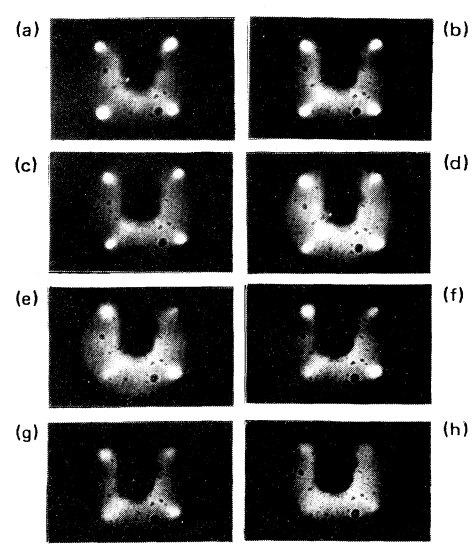

FIG. 5. LEED patterns taken during the growth of Li on the unreconstructed CdTe(100) surface at 13 eV. (a) $\theta_{Li}=0$, (b) $\theta_{Li}=0.04$, (c) $\theta_{Li}=0.08$, (d) $\theta_{Li}=0.13$, (e) $\theta_{Li}=0.33$, (f) $\theta_{Li}=0.42$, (g) $\theta_{Li}=0.67$, and (h) $\theta_{Li}=1$.

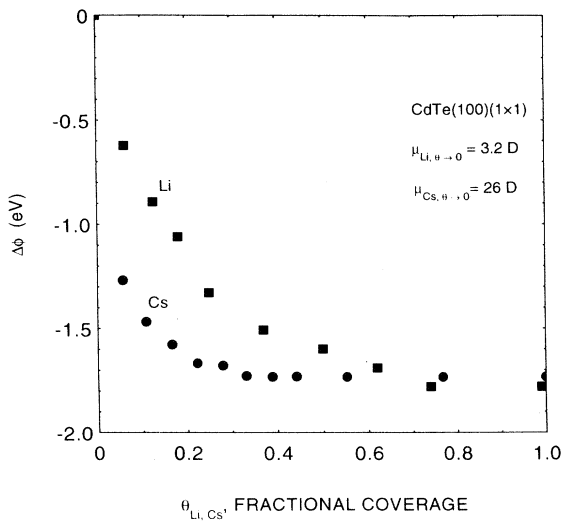

FIG. 6. Work-function lowering of CdTe(100) unreconstructed surface as a function of Li and Cs surface coverage, Cs curve from Ref. 6 given for comparison.

eV/ML, up to $\theta=0.06$, followed by a moderate decrease and a plateau beyond $\theta=0.335$, the Li curve shows an initial drop of only $d(\Delta\phi)/d\theta_{\mathrm{Li}}\approx 10.3$ eV/ML followed by a much more moderate decrease and a plateau after $\theta=0.739$. From the initial slopes of the variation of the work function with coverage, the dipole moments can be calculated using the Helmholtz equation,

$$\mu=\frac{-\Delta\phi\times 10^{18}}{2\pi n_{\mathrm{Cs,Li}}\times 300}\ , \tag{1}$$

where $\Delta\phi$ is given in volts, μ in debye, and $n_{\mathrm{Cs,Li}}$ is the number of adsorbate atoms/cm^2.

The dipole moments for cesium and for lithium per adsorbed alkali atom at the initial stages of adsorption are calculated from Eq. (1), giving 26 D and 3.2 D, respectively. Li and Cs are totally ionized at low coverages on this surface. The dipole moment for Cs is much higher than the values typically reported for Cs on metal surfaces (4–15 D).[19,20] The high dipole moments obtained for Cs on semiconductors were interpreted, (18–30 D) for GaAs,[21] as caused by a longer effective dipole length, which arises from less effective screening of the Cs^+ charge by electrons in bulk. The nonlinear variation of $\Delta\phi$ with coverage can be described by a point-depolarization model as developed by Topping[22] and which can generally be applied well to mobile adsorbates. A variation of this model as developed by MacDonald and Barlow[23] can be used for immobile adsorbates,

$$-\Delta\phi=\frac{2\pi n_a\mu_0}{1+\alpha\Lambda\Delta(n_a)^{3/2}}\ , \tag{2}$$

where n_a is the density of adsorbed atoms, in adatoms/cm^2, μ_0 is the dipole moment at infinite dilution, α is the adsorbate polarizability, Λ is a constant related to the geometry of the adsorbate atoms arrangement at the surface [$\Lambda=9.034$ for (100) surface], and $\Delta=1$ (mobile layer) and $\Delta=\theta^{-1/2}$ (immobile layer). A fit of the experimental data to both models is shown in Fig. 7. It appears that the Topping plot for the immobile-layer model gives a better fit over the entire range of coverages whereas the plot for the mobile layer fails to fit, mostly, at the initial stages of the adsorption, where the charge transfer and dipole moments are at a maximum. Using the immobile-layer model, a value of $\mu_{0,\mathrm{Cs}}=127.2$ D (Ref. 24) and $\mu_{0,\mathrm{Li}}=4.22$ D was calculated for the dipole moments at infinite dilution for Cs and for Li, respectively. Even higher values were reported in the past for Cs on GaAs (185 D).[25] A comprehensive search of the literature was made to find previous reports on the value of the dipole moments for Li on semiconductor surfaces without much success. Only one report was found which deals with Li adsorption on GaAs.[26] This work did not give any calculated values for the dipole moment. From the initial slope of the curve of work-function variation

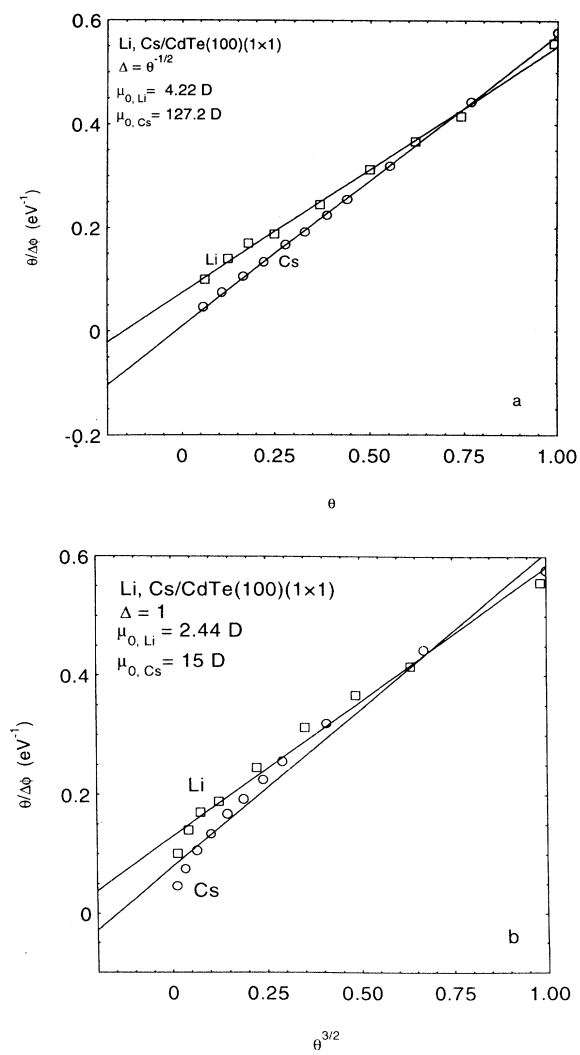

FIG. 7. Plots of $\theta/\Delta\phi$ vs (a) θ (immobile-adsorbate-layer model) and (b) $\theta^{3/2}$ (mobile-adsorbate-layer model) for both alkali species, Li and Cs.

versus Li adsorption given in their report, we can calculate a value of ~4.4 D, which agrees well with the value obtained in our work. The work-function change dependence on oxygen adsorption is shown in Fig. 8. Oxygen adsorbed on the cesiated surfaces raises the work function by 0.5 eV [Fig. 8(a)]. No difference is observed in the work-function change with oxygen exposure for $\theta_{Cs}=0.5$ or $\theta_{Cs}=1$ [Fig. 8(b)]. This indicates that the electronegative element is adsorbed on top of the cesium atoms and has a low affinity to CdTe adsorption sites and does not disrupt the existent Cs-CdTe bonds. From the work-function variation with oxygen exposure, Fig. 8(a), we see that the curve for the cesium-covered CdTe surface reaches a plateau at 60 L of oxygen exposure.

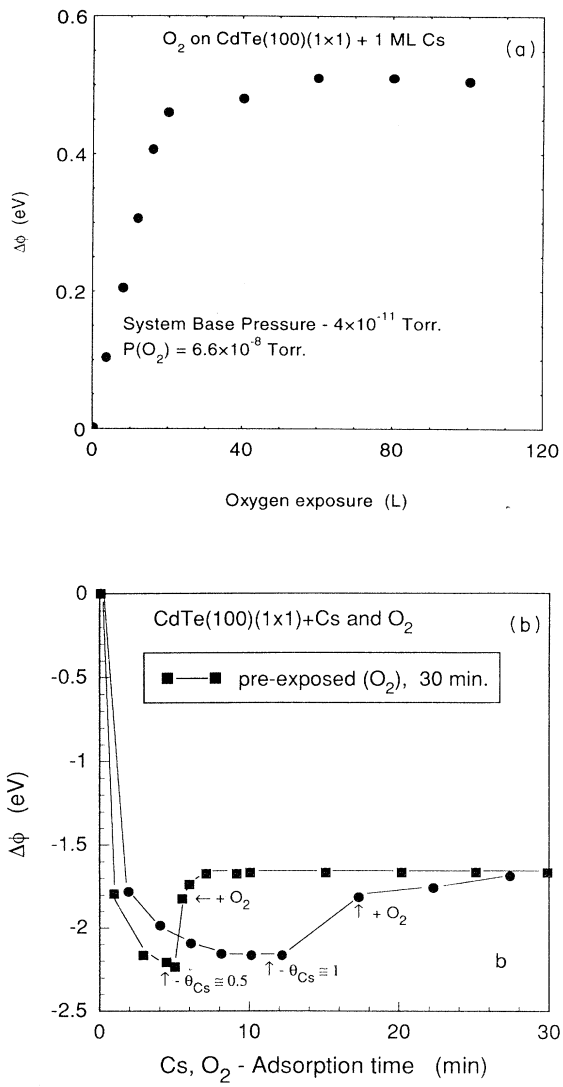

FIG. 8. (a) Work-function change of CdTe(100) unreconstructed and cesiated surface vs oxygen exposure (in Langmuirs), (b) work-function change vs oxygen exposure for ■, partially cesiated surface, and ●, completely cesiated surface.

D. Reflection electron energy loss spectroscopy of clean and cesiated surfaces: Temperature dependence

REEL spectra of the CdTe(100) unreconstructed surface were taken from the clean surface and during growth of a monolayer of Cs at room temperature. Figure 9(a) shows the loss spectra from CdTe(100)(1×1) for $E_p=100$ eV taken at different Cs coverages, $\theta_{Cs}=0-1$. The structures designated E, Cd 4d, and $\hbar\omega_p$ are of bulk origin;[27] E is a bulk interband loss, Cd 4d is due to the transition from the Cd 4d level at 10.5 eV below the valence-band maximum to a conduction-band state, and $\hbar\omega_s$ and $\hbar\omega_p$ are assigned to the surface and bulk plasmon losses, respectively. The structure called S is of surface origin. Beside the REEL structure, which was already identified in the past, a marked new peak in the lower part of the energy-loss spectrum was observed in our experiment: $S_0=2.4$ eV. Transitions in the low-energy-loss range of the spectra were not reported in the comprehensive work by Ebina and co-workers, but a similar transition was reported by Hengehold and Pedrotti[28] at $I=2.2$ eV for REEL, and at $I=2.4$ eV for transmission-electron energy loss. This structure was interpreted as having an interband transition origin. Since, according to our experiment, at very low coverage of Cs this peak in the spectrum disappears completely at $\theta_{Cs}=0.11$, it seems most probable that this peak is related to a transition in which a surface state is involved. To further investigate the origin of S_0, REEL spectra were taken at two different primary energies, $E_p=70$ and 100 eV from a clean CdTe(100)(1×1) sample and from an Ar^+ sputtered one (at 800 eV argon-ion primary energy for 10 min). In the spectra taken at low primary energy ($E_p=70$ eV), S_0 is enhanced in intensity compared to the spectra taken at higher primary energy ($E_p=100$ eV), and it is not existent at all in the spectra taken from the sputtered surface [Fig. 9(b)]. Lower primary energy (E_p) increases the cross section for surface features. This points out a surface origin for S_0 which is related to the surface order of the CdTe(100) substrate in which a specific surface state is involved. The sputtered surface is assumed to have a very high content of surface defects, therefore this specific surface state is nonexistent. A peak at 26.6 eV is clearly seen [Fig. 9(a)] already at very low coverage $\theta_{Cs}=0.06$, and is attributed to a Cs 5s core-level transition. This transition was reported in the past for other Cs/semiconductor systems.[29–31]

Due to its high partial pressure, it is not possible to grow more than one monolayer of Cs in UHV at room temperature (RT). An amount equivalent to 4–5 ML of Cs was deposited at 96 K and REEL spectra were taken immediately thereafter [Fig. 9(c)]. An energy loss $\Delta E=2.05$ eV, which is not existent at RT, is observed. It is assumed that this inelastic scattering is associated with a surface plasmon.[32] This energy loss is attributed to the 2D Cs surface plasmon ($\hbar\omega_s$) that splits with raising the temperature (this is equivalent to a thinner Cs film on the surface) towards $\omega_s^{\pm}$(Cs), that is the 2D-antisymmetric and 2D-symmetric surface-plasmon modes of the very thin Cs overlayer.[33] The shift to lower loss energies in the cesium surface plasmon ($\hbar,\omega_s$) indicates

that we are observing the symmetric branch ω_s^-. Using the classical free-electron dielectric function $\varepsilon(\omega) \sim 1-(\omega_p/\omega)^2$, the relation which describes the surface plasmons is given by

$$\omega_s^{\pm} = \frac{\omega_p}{\sqrt{2}}[1 \pm \exp(\kappa a)]^{1/2} , \quad (3)$$

where the positive and negative signs correspond to the antisymmetric and the symmetric modes of vibration, respectively, a is the thickness of the film where the plasma oscillations take place, and κ is the wave number of the disturbance. The antisymmetric mode of vibration is not revealed, in our case, because it remains hidden in the background of the bulk transitions of the substrate (very steep tail on the low-energy-loss part of the spectra). The intensity of this characteristic energy loss in inelastic scattering is reduced at higher temperatures, which is equivalent to a reduced Cs coverage of the substrate because of desorption, and it disappears completely at RT. The Cs 5s core-level transition continues to be observable with high intensity at RT indicating a sizable amount of Cs on the surface. This indicates that Cs is in a nonmetallic state on CdTe(100) at monolayer coverage. This type of behavior was also reported by other groups for Cs on GaAs.[34]

IV. SUMMARY AND CONCLUSIONS

In this work some complementary surface science spectroscopies and work-function measurements were used to investigate the adsorption of Li, Cs, and oxygen on CdTe(100). From LEED measurements on CdTe(100) we found two surface reconstructions: CdTe(100)$(3\times1)R45°$ and CdTe(100)(3×3), which are probably dependent on surface stoichiometry. From AES-LEED measurements we found that, at the monolayer range, Li and Cs grow differently. Li has a constant sticking probability all over the ML range while Cs has a variable sticking probability which is characteristic for growth of 2D islands, which coalesce at the end of the first ML. Both monolayers have an amorphous structure. Adsorption of oxygen on the cesiated surfaces increases the work function by 0.5 eV indifferently of whether the Cs surface coverage is complete, $\theta_{Cs}=1$, or half covered, $\theta_{Cs}=0.5$. This indicates that the electronegative element is adsorbed on top of the cesium atoms and has a very low affinity to CdTe adsorption sites nor disrupts existent Cs-CdTe bonds. An amount of 60 L of O_2 is sufficient to completely saturate work-function changes of a ceisated CdTe surface. The dipole moments at infinite dilution were calculated from a Topping-MacDonald-Barlow model giving $\mu_{0,Li}=4.22$ D and $\mu_{0,Cs}=127.2$ D for lithium and cesium, respective-

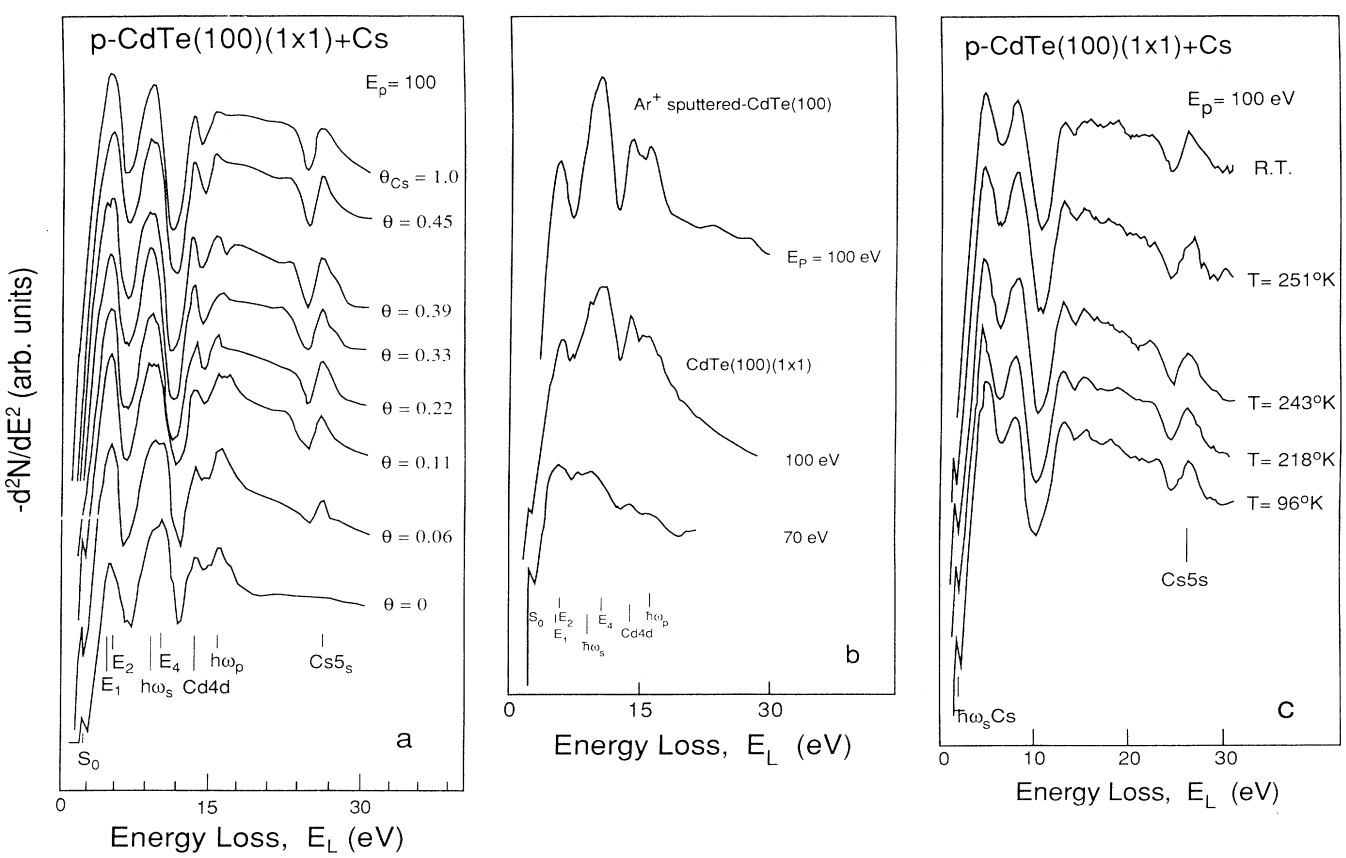

FIG. 9. REEL spectra taken as $-d^2N/dE^2$ vs energy loss (from 0 to 30 eV) of CdTe(100) unreconstructed surface: (a) during growth of Cs monolayer at $E_p=100$ eV, (b) clean CdTe(100(1×1) at $E_p=70$ and 100 eV and of Ar^+ sputtered surface at $E_p=100$ eV, and (c) REEL spectra of CdTe(100) unreconstructed surface taken at low temperatures (96–300 K) at $E_p=100$ eV.

ly. For both elements, a better fit of the experimental data was obtained when $\Delta=\theta^{-1/2}$ (immobile-layer model). The characteristic loss S_0 at 2.4 eV in REEL measurements, at room temperature, is interpreted as having a surface-related origin. The characteristic loss which is observed on the cesiated surfaces at 26.6 eV is assigned to a Cs 5*s* core-level transition. The energy loss at low temperatures (96 K), $\Delta E=2.05$ eV, is attributed to the 2D Cs surface plasmon ($\hbar\omega_s$) that shifts towards ω_s^-, the 2D symmetric mode of vibration of the Cs surface plasmon, with rising temperature. The appearance of the metallic plasmon loss only at low temperatures [when more than a monolayer of Cs is covering the surface (4–5 ML)] indicates that Cs is nonmetallic on CdTe(100) at a monolayer coverage.

ACKNOWLEDGMENTS

J.G. gratefully acknowledges the financial support by a grant from the Technion Research and Development Foundation which partially supported the experiments performed at the Technion and a grant from the Danish Natural Sciences Research Council which allowed most of the writing.

[1]R.-L. Bell, *Negative Electron Affinity Devices* (Clarendon, Oxford, 1973).
[2]J.-M. Chen and C.-A. Papageorgopoulos, Surf. Sci. **26**, 499 (1971).
[3]M. Kitson and R.-M. Lambert, Surf. Sci. **109**, 60 (1981).
[4]M. Kitson and R.-M. Lambert, Surf. Sci. **110**, 205 (1981).
[5]D. Rodway, Surf. Sci. **147**, 103 (1984).
[6]J. Gordon, H. Schechter, and M. Folman, Phys. Rev. B **49**, 4898 (1994).
[7]W.-E. Spicer, J. Appl. Phys. **12**, 115 (1977).
[8]G.-S. Almasi and A.-C. Smith, J. Appl. Phys. **39**, 233 (1968).
[9]N.-A. Foss, J. Appl. Phys. **39**, 6029 (1968).
[10]D.-C. Rodway, M.-G. Astles, and D.-R. Wight, J. Phys. D **16**, 1317 (1983).
[11]M. Chu, A.-L. Fahrenbruch, R.-H. Bube, and J.-F. Gibbons, J. Appl. Phys. **49**, 322 (1978).
[12]R. Nathan and B.-J. Opkins, J. Phys. E **7**, 851 (1974).
[13]S. Kennou, S. Ladas, and C. Papageorgopoulos, Surf. Sci. **152/153**, 1213 (1985).
[14]J. Derrien and F. Arnaud D'Avitaya, Surf. Sci. **65**, 668 (1977).
[15]J.-L. Desplat and C.-A. Papageorgopoulos, Surf. Sci. **92**, 97 (1980).
[16]M.-P. Tosi and F.-G. Fumi, J. Phys. Chem. Solids **25**, 31 (1964).
[17]M.-A. Mendez, F.-J. Palomares, M.-T. Cuberes, M.-L. Gonzales, and F. Soria, Surf. Sci. **251/252**, 145 (1991).
[18]T. Takahashi and A. Ebina, Appl. Surf. Sci. **11/12**, 268 (1982).
[19]J.-W. Gadzuk, in *The Structure and Chemistry of Solid Surfaces,* edited by G.-A. Somorjai (Wiley, New York, 1969).
[20]J. Hölzl and F.-K. Schulte, *Solid Surface Physics,* Springer Tracts in Modern Physics Vol. 85 (Springer-Verlag, Berlin, 1979).
[21]T.-E. Madey and John T. Yates, Jr., J. Vac. Sci. Technol. **8**, 39 (1971).
[22]R. Topping, Proc. R. Soc. London Ser. A **114**, 67 (1927).
[23]J.-R. MacDonald and C.-A. Barlow, Jr., J. Chem. Phys. **39**, 412 (1963).
[24]In this calculation we adhere to the convention of using a factor 2 in Eqs. (1) and (2) which refers to the image-charge model for the dipole moments. The dipole moment in Ref. 6 was given using a factor 4 for the Topping equation (center of gravity of the charges) which gives half of the value reported in this work.
[25]H.-J. Clemens, J. von Wienskowski, and W. Mönch, Surf. Sci. **78**, 648 (1978).
[26]C. Argile and G.-E. Rhead, Thin Solid Films **152**, 545 (1987).
[27]Atsuko Ebina, Kiyomitsu Asano, and Tadashi Takahashi, Phys. Rev. B **22**, 1980 (1980).
[28]R.-L. Hengehold and F.-L. Pedrotti, Phys. Rev. B **6**, 2262 (1972).
[29]J. Derrien, F. Arnaud D'Avitaya, and M. Bienfait, Solid State Commun. **20**, 557 (1976).
[30]G. Rancelov and L. Surnev, Surf. Sci. **185**, 457 (1987).
[31]M. Kiskinova, M. Tikhov, and L. Surnev, Surf. Sci. **238**, 25 (1990).
[32]E.-A. Stern and R.-A. Ferrell, Phys. Rev. **120**, 130 (1960).
[33]A.-U. MacRae, K. Müller, J.-J. Lander, J. Morrison, and J.-C. Phillips, Phys. Rev. Lett. **22**, 1048 (1969).
[34]T. Maeda Wong, D. Heskett, N.-J. Dinardo, and E.-W. Plummer, Surf. Sci. Lett. **208**, L1 (1989).

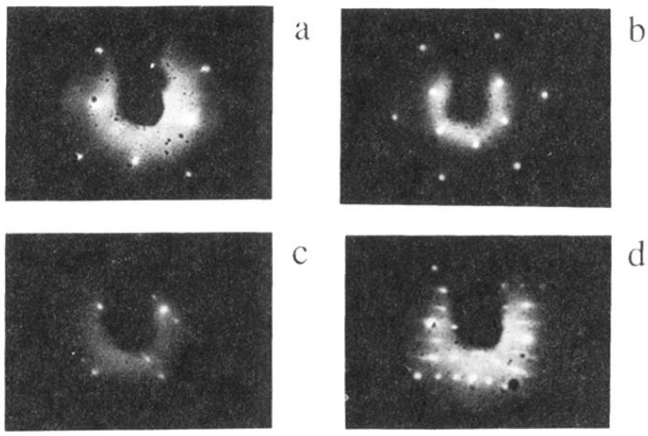

FIG. 3. (a) CdTe(100) unreconstructed surface at 40 eV, (b) CdTe(111) unreconstructed surface at 25 eV, (c) CdTe(100)$(3\times1)R45°$ at 40 eV and (d) CdTe(100)(3×3) at 40 eV.

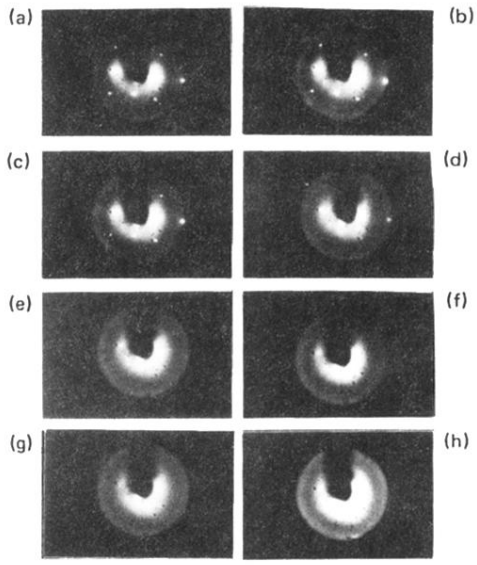

FIG. 4. LEED patterns taken during the growth of Cs on the unreconstructed CdTe(100) surface at 40 eV. (a) $\theta_{Cs}=0$, (b) $\theta_{Cs}=0.06$, (c) $\theta_{Cs}=0.11$, (d) $\theta_{Cs}=0.22$, (e) $\theta_{Cs}=0.33$, (f) $\theta_{Cs}=0.39$, (g) $\theta_{Cs}=0.50$, and (h) $\theta_{Cs}=1$.

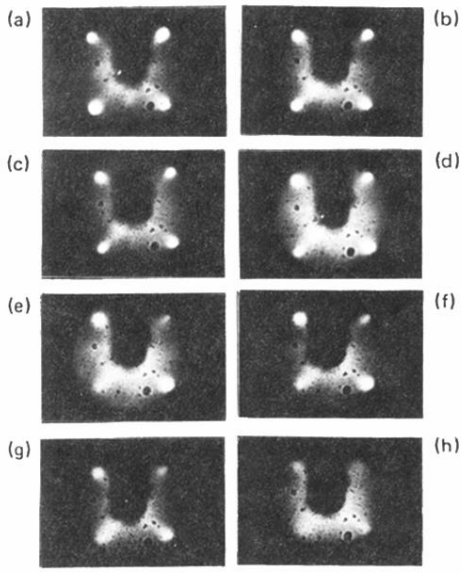

FIG. 5. LEED patterns taken during the growth of Li on the unreconstructed CdTe(100) surface at 13 eV. (a) $\theta_{Li}=0$, (b) $\theta_{Li}=0.04$, (c) $\theta_{Li}=0.08$, (d) $\theta_{Li}=0.13$, (e) $\theta_{Li}=0.33$, (f) $\theta_{Li}=0.42$, (g) $\theta_{Li}=0.67$, and (h) $\theta_{Li}=1$.